

Heat transmission during thermal shock testing of ceramics

T. NISHIKAWA, T. GAO, M. HIBI, M. TAKATSU

Department of Materials Science and Engineering, Nagoya Institute of Technology, Gokiso-cho, Showa-ku, Nagoya 466, Japan

M. OGAWA

Japan Fine Ceramics Center, Mutsuno 2-4-1, Atsuta-ku, Nagoya 456, Japan

The thermal shock resistance of ceramics is generally evaluated by the water-quench test, in which it is important and necessary to understand the heat-transmission behaviour. A novel and simple method for measuring the transitional changes of temperatures in ceramics has been proposed. Changes in temperature at two different positions in zirconia ceramics were measured to estimate the temperature distribution. From the analytical results, it was clear that the heat-transmission behaviour changed with the quenching temperature or water temperature. The Biot number also changed remarkably with time or with the surface temperature in this experiment. These results are useful in practice for examining the cooling conditions in the thermal shock test.

1. Introduction

A number of methods has been proposed to evaluate the thermal shock resistance of ceramics. In particular, the water-quench test has been used frequently, in which the relationship between a critical temperature difference and thermal/physical properties of material is also discussed. However, some problems with this method have been pointed out and other methods were recommended recently [1, 2]. A significant disadvantage is the difficulty of accurately monitoring the heat-transfer condition. Therefore, a small variation in the test procedure can cause large variations in results. A few studies have investigated the heat-transfer coefficient, which is important to understand the above conditions [3]. It is difficult to obtain an adequate heat-transfer coefficient in water-quenching, owing to the heat transmission near the boiling temperature or rapid change of surface temperature [4]. In general, the critical temperature difference, $\Delta\theta_c$, which causes a significant decrease in the retained strength, is defined as the thermal shock resistance of the material. The maximum thermal stress is generated in the specimen and thermal stress cracking or fracture is observed at that time. Therefore, it is desirable to obtain a heat-transfer coefficient at maximum thermal stress, which reflects the cooling conditions.

In this study, the specimen was prepared with a shape to maintain the condition of one-dimensional heat conduction during water quenching. Transient temperatures in the specimen were measured continuously. An average heat-transfer coefficient was estimated from the temperature distribution at the maximum thermal stress in the specimen. The experimental difference, based on equipment or quen-

ching conditions, can also very easily be examined and determined, if a standard specimen is prepared using this method.

2. Experimental procedure

2.1 Specimen preparation

The transient temperatures were measured continuously at two different positions in the specimen using the following procedures. The dimensions and shape of the specimen are illustrated in Fig. 1. Three ceramic

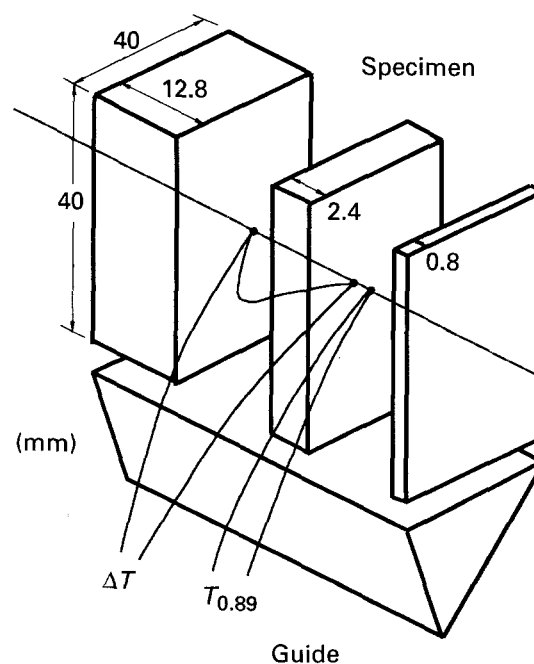


Figure 1 Dimensions and shape of the specimen.

plates of different thickness (12.4, 2.4 and 0.8 mm) were prepared in layers, a thermocouple was inserted at ξ_1 , and a double-thermocouple was used between ξ_1 and ξ_2 positions. The temperature distribution of the specimen perpendicular to the layer was estimated. The non-dimensional length, ξ , is expressed as $\xi = x/l$, where x is the length from the centre of the specimen and l is one-half the thickness of the specimen. $\xi_1 = 0.61$ and $\xi_2 = 0.88$ in this experiment. The ceramic plates were lapped to a mirror finish and grooved to insert the thermocouple. A set of ceramic plates was secured with wire after spreading ceramic paste to prevent water penetration. Another thermocouple was attached at a short distance from the surface of the specimen to obtain exactly the immersion time in water. A trigonal prism made of ceramics was added as a guide at the bottom of the specimen to minimize adherent bubbles on the specimen surface. Commercial ceria-doped tetragonal zirconia ceramics [5], whose heat conductivity does not change over a wide temperature range, were used as the specimens. The thermal and physical properties are listed in Table I.

2.2. Transient temperature measurement

After heating uniformly at a given furnace temperature, the specimen was immersed in a water bath. The drop height was fixed at 30 cm maximum, to prevent cooling of the specimen during dropping. The volume of the water bath, whose temperature was controlled at 0, 25, 60 or 90 °C, was 10 l. The temperature was maintained so that water and ice could coexist at 0 °C or by heating with a pipe heater at 60 or 90 °C without stirring. The transient temperatures at two positions were stored continuously as data in the digital storage oscilloscope every 5 ms. The observed data were the average value of 50 data points. The measuring was conducted for a maximum of 10 s, with due consideration for the time to generate maximum thermal stress.

3. Results and discussion

The observed changes of temperatures obtained as above, were arranged by the following method. For the zirconia ceramics used in this experiment, the changes of thermal conductivity at the developed temperature can be ignored. The shape of the specimen is regarded as an infinite plate for calculation.

TABLE I Thermal and physical properties of ceria-doped tetragonal zirconia ceramic

Property	Value
Density (g cm^{-3})	6.18
Flexural strength (MPa)	506
Weibull's modulus	68.1
Fracture toughness ($\text{MPa m}^{0.5}$)	18.9
Young's modulus (GPa)	196
Thermal conductivity ($\text{cal cm}^{-1} \text{s}^{-1} \text{K}^{-1}$) at $RT \sim 800^\circ\text{C}$	0.007
Thermal expansion coefficient ($\times 10^{-6} \text{K}^{-1}$)	9.0
Specific heat ($\text{cal g}^{-1} \text{K}^{-1}$)	0.13

From these facts, we may express the following thermal conduction equation assuming a constant Biot number independent of temperature

$$\partial^2 T^*/\partial \xi^2 = \partial T^*/\partial \eta \quad (1)$$

$$T^* = 1 \quad \text{at } \eta = 0 \quad (2a)$$

$$\partial T^*/\partial \xi = 0 \quad \text{at } \xi = 0 \quad (2b)$$

$$-\partial T^*/\partial \xi = \beta T^* \quad \text{at } \xi = 1 \quad (2c)$$

The solution may be written

$$T^* = 2\beta \sum_{n=1}^{\infty} \exp(-\delta_n^2 \eta) \cos \delta_n \xi / (\beta^2 + \beta + \delta_n^2) \cos \delta_n \quad (3)$$

where δ_n is the n th positive solution of $\delta \tan \delta = \beta$. T^* is the non-dimensional temperature shown as $(\theta - \theta_f)/(\theta_i - \theta_f)$, where θ is the temperature and the subscripts i and f are the initial and final condition, respectively, β is the Biot number shown as hl/λ , where h is the thermal transfer coefficient, l is the half-width of the specimen and λ is the thermal conductivity. η is a Fourier number shown as $\kappa t/l^2$, where κ is thermal diffusivity and t is time.

The temperature distribution in the specimen with time can be calculated theoretically. By substituting the values of the Biot number into Equation 3, the calculated temperature distribution is obtained and shown in Fig. 2 together with the observed data. These calculations were done automatically by a personal computer. The observed data in the early stage after quenching did not agree with the calculated temperature distribution, but they did so as the time approached that for maximum thermal stress on the surface of the specimen. In this case, the Fourier number does not always agree between observed and calculated values. The temperature distribution can be expressed and estimated easily by this method, using the corresponding Biot number.

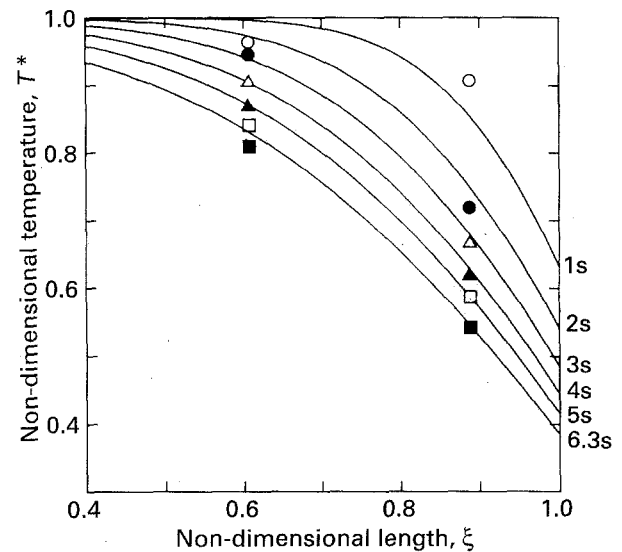


Figure 2 Calculated temperature distribution and observed temperature for the specimen quenched from 205 °C to 25 °C. The maximum indicates the time at which the maximum thermal stress was generated, assuming $\beta = 4$. Observed temperature: \circ 1 s, \bullet 2 s, \triangle 3 s, \blacktriangle 4 s, \square 5 s, \blacksquare 6.3 s.

The measuring positions must be decided, at which the marked temperature difference is obtained at various Biot numbers. Fig. 3 shows the temperature distribution for the specimen, calculated at the maximum thermal stress, assuming a constant Biot number. The measuring positions in this experiment were $\xi_1 = 0.61$ and $\xi_2 = 0.88$. At these positions, one or two significant figures can be obtained within 10°C and a distance of 0.1 mm . The non-dimensional temperature at $\xi = 0$ was considered to be 1.0 . The starting time of measurement was decided from the temperature obtained by another thermocouple above the surface. Therefore, the decrease of temperature while falling in air was ignored. It did not affect the estimation of the Biot number.

The thermal transmission can be presumed and discussed from the changes of temperatures. The transient temperatures at two positions were previously estimated from Equation 3 assuming a constant Biot number. Then, the observed data for the normalized non-dimensional temperature were plotted. Fig. 4a shows the case of quenching from 205°C to 25°C and Fig. 4b shows the case for quenching from 180°C to 0°C . The quenching temperature differences were equal to 180°C in both cases. The dotted curve in Fig. 4 is for the non-dimensional temperatures at a maximum thermal stress dependent on each Biot number, which is estimated from Equations 3 and 5, as described below.

Comparing the observed and calculated data, a marked increase of Biot number is observed immediately after quenching, and the observed data located on one curve have almost the same Biot number. The observed data can be divided into three regions: in the first region (Region A), the observed data showed a sudden change without a constant Biot number, indicating that the formed or adherent bubbles on the specimen surface significantly affect the heat transmission. The Fourier number in this region is $0.02\text{--}0.04$, small for every condition. The volume of bubbles may be related to the surface roughness of the specimen. In

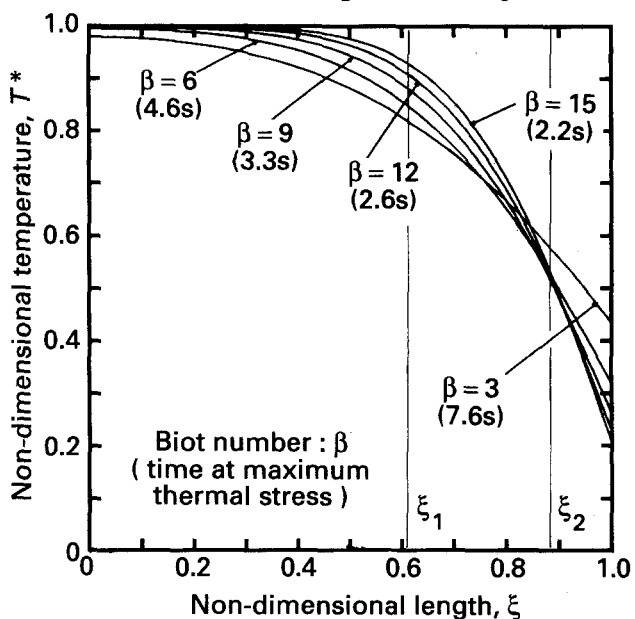


Figure 3 Calculated temperature distribution at the maximum thermal stress in the specimen, assuming a constant Biot number.

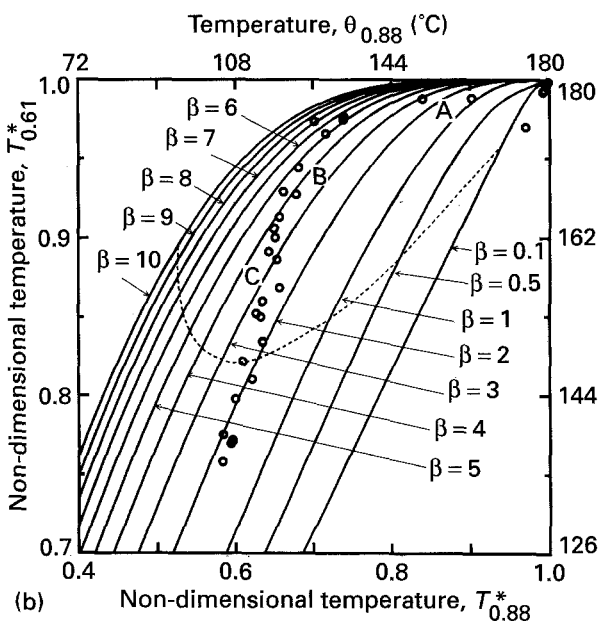
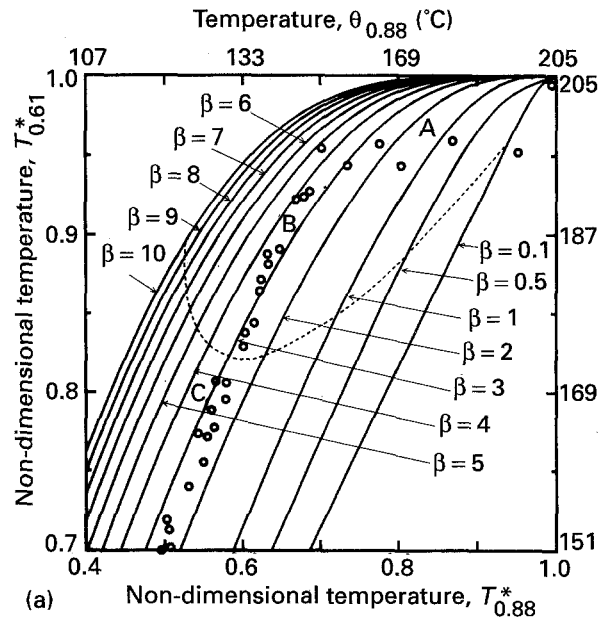


Figure 4 Transient non-dimensional temperature at two positions (ξ_1, ξ_2) plotted against the calculated change of temperature with constant Biot number: (a) quenched from 205°C to 25°C ; (b) quenched from 180°C to 0°C . (O) Observed data.

particular, the data in this region are influenced by the dropping method. In the next region (Region B), the boundary formed by bubbles had a constant thickness and the heat transmission was in the steady-state, with a constant Biot number. In Region C, the temperature of the surface fell below 100°C and natural convection is predominant. In particular, a marked decrease of Biot number was observed (Fig. 4b).

In Region A, the heat transmission is in an unsteady state, judging from the change of data in Fig. 4. The heat-transfer coefficient in this region cannot be obtained. Numerical calculation of the heat transmission becomes complicated, even if one assumes that the Biot number is a function of temperature to determine the heat-transfer coefficient. In practice, thermal stress produced in the specimen did not become large enough to cause fracture in this region because of the formed or adherent bubble shield.

The thermal stress in the specimen is closely connected with the transitional temperature distribution. However, the thermal stress is expressed by

$$\sigma^* = \int_0^1 T d\xi - T \quad (4)$$

If the temperature distribution at a given time is estimated, thermal history may be ignored in this equation. Therefore, it is most important to determine the temperature distribution at maximum thermal stress in the experimental thermal shock test. In the present work, a simple method to estimate the Biot number at maximum thermal stress has been proposed. The maximum thermal stress was expressed as a function of Biot number independent of time, as follows

$$1/\sigma_{\max}^* = a + b/\beta \quad (5)$$

where a and b are experimental constants at 1.5 and 3.25, respectively [6–7]. The non-dimensional maximum thermal stress, σ_{\max}^* , exhibits $R/\Delta\theta_c$, where R is the thermal stress resistance parameter and $\Delta\theta_c$ is the critical temperature difference. The observed data in Fig. 4 showed the non-dimensional temperature at ξ_1 and ξ_2 in the specimen. If the temperature distribution at maximum thermal stress is presumed, an adequate Biot number is obtained at that time. Therefore, heat-transmission conditions can be expressed using only two different temperatures in the thermal shock test. The disagreement between the calculated Fourier numbers and those observed, caused the difference of time at maximum thermal stress. In this experiment, the temperature distribution did not obey the boundary conditions in Equation 2 and the Biot number became a function of temperature in Region A. With increasing time, the temperature distribution was approximated by the curve having a constant Biot number in Region B. The experimental error in the estimation of the Biot number is less, except that the thermal stress approaches the maximum value or the Biot number becomes remarkably large in Region A. The number of circles shows the period consumed at every region. For the case in Fig. 4a, the real time in Region A was 1.5 s, 1.5 s in Region B and above 3.0 s in Region C.

For the next analytical step, one value of the Biot number in Region B must be used for calculation of the heat-transfer coefficient. As the Biot number became almost constant from the initial bending point

(Region A–B) in Fig. 4, it can be also estimated by assuming that the temperature at a given point in the figure is the initial condition. This calculation indicated that slightly more time was necessary to reach the maximum thermal stress. However, the change of Biot number in the steady region, B, was small and there was no effect on its estimation, even though the time at maximum thermal stress was not obtained exactly. In Region C, controlled by natural convection, the Biot number and the heat-transfer coefficient became low with time.

As a consequence, the effective heat-transfer coefficient in the thermal shock test was calculated from the Biot number in Region B. The Biot number and heat-transfer coefficient at each thermal shock test are listed in Table II, together with the initial or final Fourier number of Region B. During quenching into the water bath at 0 °C, the Biot numbers differed with quenching temperature. The calculated heat-transfer coefficient was $1.1\text{--}2.9 \times 10^3 \text{ W m}^{-2} \text{ K}^{-1}$. On the other hand, for quenching at other temperatures, the relatively constant heat-transfer coefficient was obtained from $1.5\text{--}2.0 \times 10^3 \text{ W m}^{-2} \text{ K}^{-1}$, with the same quenching temperature difference. In general, the heat-transfer coefficient in the thermal shock test is affected significantly by the surface temperature of the specimen [8]. If the quantity of heat given by the specimen became equal to that which escaped from the surface to the water, the heat transmission was in the steady state. Therefore, the heat-transfer coefficient in this experiment did not change remarkably except for the initial region after quenching, in contrast to the data calculated from the residual strength in the quenching test [3].

The data in Region C, in which the heat transmission was dominated by natural convection, were applied following equation [9] for the examination of the experimental results. The average heat-transfer coefficient was calculated from the following equation

$$\text{Nu} = 0.638 (\text{Pr Gr})^{1/4} [\text{Pr}/(0.861 + \text{Pr})]^{1/4} \quad (6)$$

where Nu is the Nusselt number shown as $\text{Nu} = hl/\lambda$, λ is the average heat conductivity of water, Pr is the average Prandtl number of water. The Grashof number, Gr, is expressed as $\text{Gr} = l^3 g \beta (\theta_w - \theta_0)/\nu^2$, where g is the gravitational conversion factor and β is the average cubical expansion coefficient of water. θ_w and θ_0 are the surface temperature of the specimen and the water temperature, respectively, ν is the kinematic

TABLE II Fourier number, η , Biot number, β , and heat-transfer coefficient, h , under various quenching conditions

	Quenching temperature (°C)					
	180	210	220	205	240	270
Water temperature (°C)	0	0	0	25	60	90
Quenching temperature difference (K)	180	210	220	180	180	180
Fourier number, η , of Region A to Region B	0.02	0.02	0.04	0.04	0.02	0.04
Biot number, β , Region B	5.5	8.0	3.0	4.0	5.0	4.5
Heat-transfer coefficient, Region B ($\times 10^3 \text{ W m}^{-2} \text{ K}^{-1}$)	2.0	2.9	1.0	1.5	1.8	1.6
Fourier number, η , of Region B to Region C	0.04	0.04	0.06	0.06	0.06	0.08

viscosity coefficient of water. The calculated heat-transfer coefficient in the above experimental equation is approximately $1 \times 10^3 \text{ W m}^{-2} \text{ K}^{-1}$. This value is smaller than that in Region B but similar to those in Region C.

An estimated Biot number is required to check against thermal or mechanical properties of the specimen. The thermal stress resistance parameter $R (= \sigma_{\max}^* \Delta\theta_c)$ is calculated from the Biot number in this experiment and the critical temperature difference $\Delta\theta_c$. Using the Biot number given in Table II and $\Delta\theta_c = 290^\circ\text{C}$ with reference to zirconia ceramics [10], R calculated from Equation 5 was found to be 112°C at $\beta = 3$ and 152°C at $\beta = 8$. On the other hand, R can be expressed as $(1 - \nu)\sigma_{\max}/E\alpha$ under quenching conditions [7], and thus may be calculated from the thermal and mechanical properties in Table I, assuming σ_{\max} is equal to tensile strength and approximately two-thirds of the bending strength. The R value at room temperature is 130°C and agrees relatively well with the above values, although the temperature dependence is ignored. Therefore, the estimated thermal transfer coefficient is useful in the thermal shock test.

4. Conclusions

The heat-transmission behaviour of ceramics during water quenching has been discussed.

1. A novel and simple method for measuring the transitional changes of temperatures in ceramics has been proposed. The changes of temperatures at two different positions in specimen were measured using a thermocouple and a double-thermocouple.

2. The observed data were plotted in a diagram, in which the transitional temperatures at two positions were previously estimated with a constant Biot number from an equation for one-dimensional heat conduction.

3. By calculating the maximum thermal stress in the specimen, the apparent heat-transfer coefficient can be estimated for a water quench.

References

1. G. A. SCHNEIDER and G. PETZOW, *J. Am. Ceram. Soc.* **74** (1991) 98.
2. W. P. ROGERS and A. F. EMERY, *J. Mater. Sci.* **27** (1992) 146.
3. P. F. BECHER, D. LEWIS, K. R. CARMAN and A. C. GONZALEZ, *Ceram. Bull.* **59** (1980) 542.
4. J. R. SINGH, J. R. THOMAS and D. P. H. HASSELMAN, *J. Am. Ceram. Soc.* **63** (1980) 140.
5. K. TSUKUMA and M. SHIMADA, *J. Mater. Sci.* **20** (1985) 1178.
6. S. S. MANSON and R. W. SMITH, *Trans. ASME* **78** (1956) 533.
7. D. LEWIS, *J. Am. Ceram. Soc.* **63** (1980) 713.
8. G. HIERL and W. WARTENBERG, *Glastech. Ber.* **62** (1989) 158.
9. E. SCHMIDT and W. BECKMANN, *Tech. Mech. Thermodynamic* **1** (1930) 341, 391.
10. M. ISHITSUKA, T. SATO, T. ENDO and M. SHIMADA, *J. Mater. Sci. Lett.* **24** (1989) 4057.

Received 9 November 1992
and accepted 29 April 1993